

# Long-Term Metabolic Correction of Phenylketonuria by AAV-Delivered Phenylalanine Amino Lyase

Rui Tao,<sup>1</sup> Lin Xiao,<sup>2</sup> Lifang Zhou,<sup>1</sup> Zhaoyue Zheng,<sup>2</sup> Jie Long,<sup>1</sup> Lixing Zhou,<sup>2</sup> Minghai Tang,<sup>1</sup> Biao Dong,<sup>2</sup> and Shaohua Yao<sup>1</sup>

<sup>1</sup>State Key Laboratory of Biotherapy and Cancer Center, West China Hospital, Sichuan University, Chengdu, Sichuan 610041, China; <sup>2</sup>National Clinical Research Center for Geriatrics, State Key Laboratory of Biotherapy, West China Hospital, Sichuan University, Chengdu, Sichuan, China

**Phenylketonuria (PKU) is an inherited metabolic disorder caused by mutation within phenylalanine hydroxylase (PAH) gene. Loss-of-function of PAH leads to accumulation of phenylalanine in the blood/body of an untreated patient, which damages the developing brain, causing severe mental retardation. Current gene therapy strategies based on adeno-associated vector (AAV) delivery of PAH gene were effective in male animals but had little long-term effects on blood hyperphenylalaninemia in females. Here, we designed a gene therapy strategy using AAV to deliver a human codon-optimized phenylalanine amino lyase in a liver-specific manner. It was shown that PAL was active in lysing phenylalanine when it was expressed in mammalian cells. We produced a recombinant adeno-associated vector serotype 8 (AAV8) viral vector expressing the humanized PAL under the control of human antitrypsin (hAAT) promoter (AAV8-PAL). A single intravenous administration of AAV8-PAL caused long-term correction of hyperphenylalaninemia in both male and female PKU mice (strain Pah<sup>enu2</sup>). Besides, no obvious liver injury was observed throughout the treatment process. Thus, our results established that AAV-mediated liver delivery of PAL gene is a promising strategy in the treatment of PKU.**

## INTRODUCTION

Phenylketonuria (PKU) is a common hereditary metabolic disorder that affects 1/4,000–40,000 live births worldwide.<sup>1</sup> PKU is inherited in an autosomal recessive pattern and is mainly caused by mutations in the gene encoding phenylalanine (Phe) hydroxylase (PAH), the enzyme catalyzing the conversion of Phe to tyrosine.<sup>2</sup> Deficiency of PAH results in the accumulation of different degrees of Phe and its metabolites, which are especially harmful for the brain, resulting in variable mental retardation and impairments when untreated.<sup>2</sup> Importantly, in pregnant PKU women, uncontrolled hyperphenylalaninemia (HPA) may result in maternal PKU syndrome, including fatal microcephaly, growth retardation, developmental delay, and congenital heart disease.<sup>2</sup>

Current treatment of PKU mainly relies on the dietary limitation in Phe, which will prevent HPA and thus the syndrome.<sup>3</sup> However,

this strategy involves a major alteration of lifestyle, and dietary limitation can also be associated with deficiencies of other necessary nutrients.<sup>4</sup> Recently, adeno-associated vector (AAV)-mediated PAH gene therapies have achieved nearly complete correction of HPA and reversal of HPA-related syndromes in animals without dietary Phe limitation.<sup>5–10</sup>

Alternatively, enzyme substitution therapy with the phenylalanine ammonia lyase (PAL) can also achieve correction of HPA and reversal of HPA-related syndromes in PKU mice. PAL proteins are a group of non-mammalian-derived Phe metabolic enzymes that lyse Phe into ammonia and *trans*-cinnamic acid.<sup>11,12</sup> Unlike PAH, PALs do not require any coenzymes when catalyzing the reaction, which make it a good candidate for PAH substitution.<sup>13</sup> In mouse models, injection of PEGylated PAL significantly lowered Phe levels in both blood and brain tissue, resulting in reduced manifestations associated with PKU, including reversal of PKU-associated hypopigmentation and enhanced animal health.<sup>14–18</sup> Among the tested PALs that derived from different species and harbored various mutations, *Anabaena variabilis* PAL (AvPAL) with C503S and C565S mutations was the most stable one during thermo and proteinase challenging.<sup>19</sup> Currently, human clinical trials with AvPAL enzymes as a treatment for PKU are ongoing.<sup>17,20</sup> However, strategies based on PAL protein therapy required weekly repeated and lifelong injection, which is challenging for patient compliance. More importantly, immune response to PAL protein also remained a big concern.<sup>17,19–22</sup>

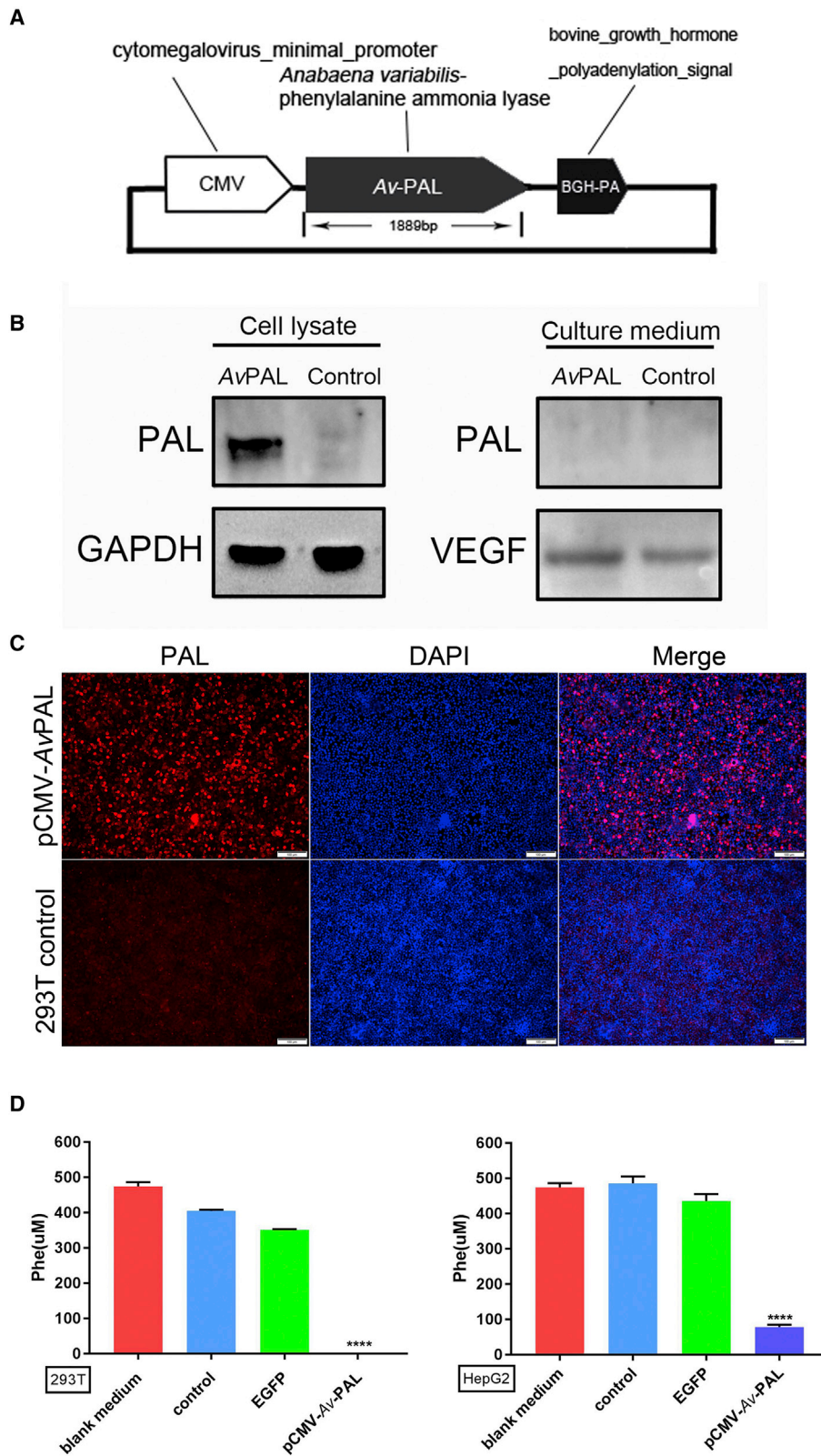
Here, we sought to deliver a humanized PAL gene to the liver of PKU mice to correct HPA. We demonstrated that PAL protein is also active

Received 28 July 2019; accepted 27 December 2019;  
<https://doi.org/10.1016/j.omtm.2019.12.014>.

**Correspondence:** Shaohua Yao, PhD, State Key Laboratory of Biotherapy and Cancer Center, West China Hospital, Sichuan University, No. 17, Section 3, Renmin Road South, Chengdu, Sichuan 610041, China.  
**E-mail:** [shaohuayao@scu.edu.cn](mailto:shaohuayao@scu.edu.cn)

**Correspondence:** Biao Dong, PhD, National Clinical Research Center for Geriatrics, State Key Laboratory of Biotherapy, West China Hospital, Sichuan University, No. 17, Section 3, Renmin Road South, Chengdu, Sichuan 610041, China.  
**E-mail:** [biaodong@scu.edu.cn](mailto:biaodong@scu.edu.cn)





(legend on next page)

when it is expressed in mammalian cells and efficiently removes extracellular Phe. A single intravenous administration of AAV8-PAL caused long-term correction of HPA in both male and female PKU mice. Our results established that AAV-mediated liver delivery of PAL gene could be a promising strategy in the treatment of PKU.

## RESULTS

### PAL Is Active in Mammalian Cells

Although PAL protein is efficient in the clearance of blood Phe when it was supplemented by subcutaneous injection, it is not known whether PAL protein is also active when it is expressed in cells. As an initial step toward PAL-based gene therapy, we tested whether PAL proteins were able to be functionally expressed in mammalian cells to remove extracellular Phe. As shown in Figure 1A, we designed a human codon-optimized PAL gene and put it into a mammalian expression plasmid in which expression PAL was controlled by cytomegalovirus (CMV) promoter. 293T cells were transfected with this plasmid, and the expression of PAL protein was confirmed by western blot and immunostaining with a PAL-specific primary antibody (Figures 1B and 1C). Importantly, PAL protein was detected only in the cell lysate, but not in the culture medium, suggesting that PAL was not secreted outside the cell. To determine the activity of intracellularly expressed PAL proteins, we tested Phe contents in culture medium through liquid chromatography-mass spectrometry (LC-MS). As we expected, pCMV-PAL transfection led to significant clearance of extracellular Phe. A similar phenomenon was also observed in liver cell line HepG2 (Figure 1D). These results suggested that depletion of intracellular Phe by PAL protein promoted cells to uptake and exhaust extracellular Phe, demonstrating the potential of PAL in gene therapy.

### Correction of HPA in Male Mice

After establishing that PAL was active when expressed in cells *in vitro*, we test whether PAL was also active *in vivo*. We constructed AAV8-PAL vector, which directs the expression of PAL with a liver-specific human antitrypsin (hAAT) promoter and apolipoprotein A enhancer (ApoE) (Figure 2A). Three groups of 4- to 8-week-old male PKU mice received AAV8-PAL at a dose of  $4 \times 10^{12}$ ,  $4 \times 10^{11}$ , and  $5 \times 10^{10}$  viral particles per mouse. PBS treatment of PKU mice of the same age were used as negative controls.

Two weeks after gene transfer, blood Phe level in  $4 \times 10^{12}$  viral particles-treated male mice significantly decreased from  $2,708 \pm 849$  to  $32 \pm 3.2 \mu\text{M}$  (Table S1), which was even lower than that in wild-type (WT) or heterozygous animals ( $99 \pm 44 \mu\text{M}$ , blood Phe of WT male mice,  $n = 18$ ; Table S3). Moreover, blood Phe concentrations in two of the three PAL-treated mice were maintained at normal

levels ( $99 \pm 44 \mu\text{M}$ ) during the whole experimental period of at least 24 weeks (Figure 2B). After 14 weeks of treatment, blood Phe began to rise in another male mouse; after 16 weeks, its blood Phe stabilized at about 40% of the pretreatment level (Table S2). As compared with PBS-treated mice, only mild reduction of Phe levels was observed in mice that received  $4 \times 10^{11}$  and  $5 \times 10^{10}$  viral particles (Figure 2B). Together, these results demonstrated the feasibility of AAV8-PAL-mediated gene therapy against HPA.

Due to attenuated biosynthesis of melanin, hypopigmentation is one of the visible phenotypes of HPA. This phenotype was nearly completely reversed in *Pah<sup>enu2-/-</sup>* mice that received  $4 \times 10^{12}$  viral particles. As early as 2 weeks after viral injection, high-dose-treated PKU mice showed noticeably darker color than untreated ones (Figure 2C). From 8 weeks on, they became indistinguishable from WT mice. However, in mice that received  $4 \times 10^{11}$  and  $5 \times 10^{10}$  viral particles, no such phenotypic rescues were observed.

After 24 weeks posttreatment, all mice were sacrificed, and liver samples were collected for analyzing the expression of transgene. Immunofluorescence staining revealed that liver samples from the  $4 \times 10^{12}$  group had over 20% PAL-positive hepatocytes. Samples from the  $4 \times 10^{11}$  group had less than 3% positive hepatocytes, whereas rare positive cells were observed in the  $5 \times 10^{10}$  group (Figure 2D). The dose-dependent expression of the PAL transgene in mice that received various dosages of AAV8-PAL was coincident with the amount of blood Phe decrease.

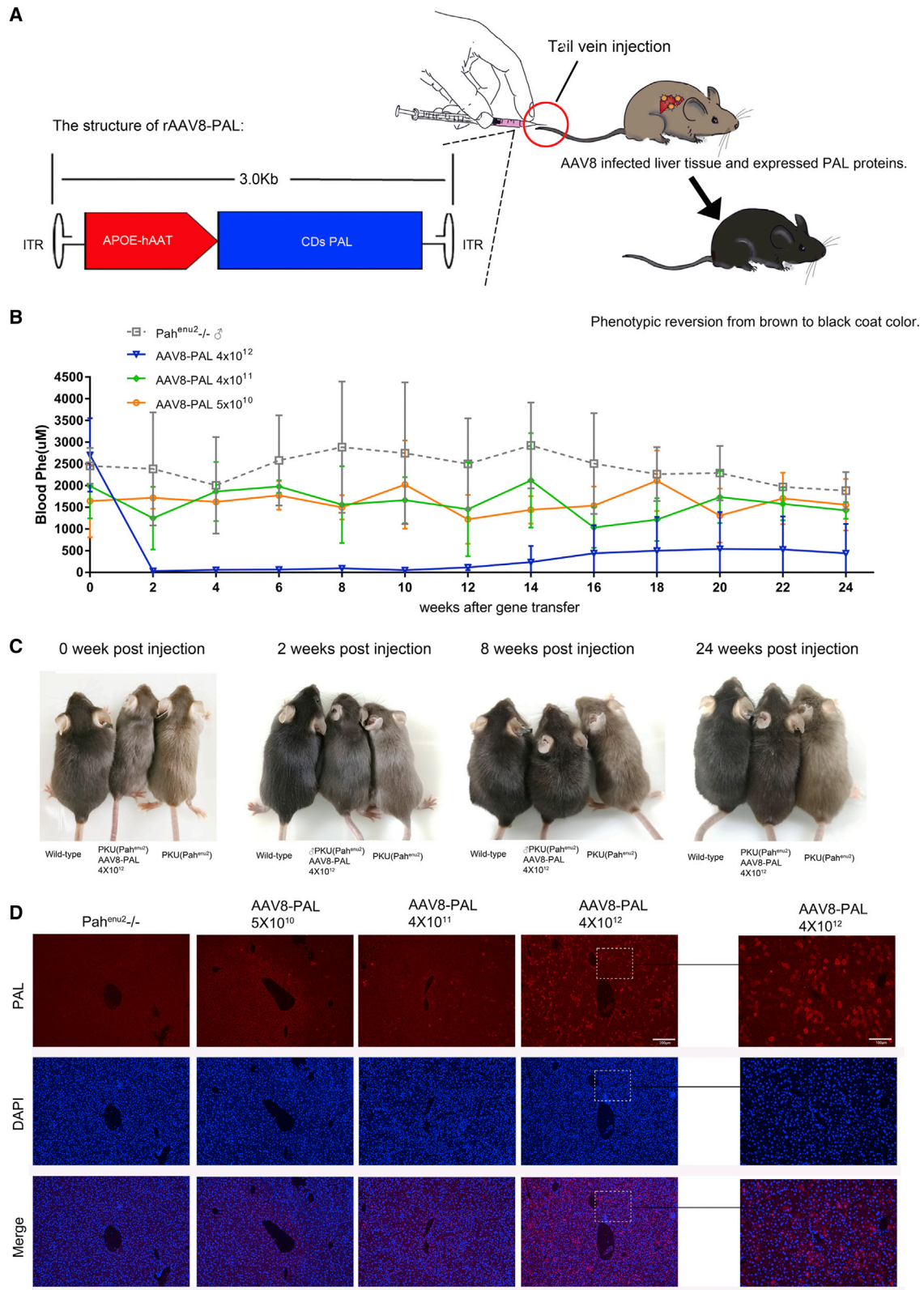
### Correction of HPA in Female Mice

Encouraged by the therapeutic effects of PAL gene therapy in male mice, we next tested the effects of AAV8-PAL in female mice. Again, three 4- to 8-week-old female PKU mice were grouped and received  $4 \times 10^{12}$ ,  $4 \times 10^{11}$ , and  $5 \times 10^{10}$  viral particles per mouse, respectively. Similar to male mice, the female mice that received a high dosage of AAV8-PAL had significantly reduced blood Phe. Two weeks after virus injection, blood Phe in mice injected with  $4 \times 10^{12}$  viral particles decreased from  $2,825 \pm 414$  to  $47 \pm 7.7 \mu\text{M}$  (Table S2), which was even lower than that in WT or heterozygous females ( $113.3 \pm 45.6 \mu\text{M}$ ;  $n = 26$ ; Table S3). Two of them maintained their Phe level at nearly normal range throughout the experimental time window of at least 24 weeks. The third began to show a gradually increasing level from 12 weeks, and its blood Phe was stabilized at about 60% of the pretreatment level. Phenotypically, the high-dose group female mice became darker at 2 weeks posttreatment as compared with PBS-treated PKU mice. The one with incomplete Phe clearance began to show brown hair at 10 weeks. Similar to the therapeutic effects observed on male mice, mice that received

### Figure 1. PAL Protein Expressed in Mammalian Cells Is Active for Clearing Extra-cellular Phe

(A) Schematic diagram of the structure of mammalian PAL plasmid. PAL derived from *Anabaena variabilis* was codon humanized and constructed into mammalian expression vector under the control of the CMV promoter. (B) Western blot results showed that PAL protein was expressed in pCMV-PAL-transfected cells; PAL protein was not detected in the culture medium of pCMV-PAL-transfected cells. VEGF served as a positive control for secreted proteins. (C) Immunofluorescence staining of the cells transfected with pCMV-PAL plasmids (scale bars, 100  $\mu\text{m}$ ). (D) LC-MS detection of Phe concentration in the cell culture medium. PAL transfection significantly reduced Phe concentration in culture medium, whereas EGFP plasmid did not (data are represented as mean  $\pm$  SD; \*\*\*\* $p < 0.0001$ ).





(legend on next page)

$4 \times 10^{11}$  and  $5 \times 10^{10}$  viral particles had only a mild decrease in Phe concentration, and no obvious phenotypic rescue was observed in these two groups. The immunofluorescence stain of transgene expression in female mice was similar to that of male mice (Figure 3C).

#### AAV8-PAL Caused No Obvious Hepatotoxicity

Considering that PAL-mediated metabolism of Phe produced trace amounts of ammonia and *trans*-cinnamic acid that are low toxicity, we next tested whether PAL gene therapy caused liver toxicity. We noted that AAV-PAL injection did increase the serum levels of alanine aminotransferase (ALT) and aspartate aminotransferase (AST) at 2 weeks postinjection, which was consistent with a previous observation that AAV infusion transiently induced elevations of ALT and AST at 2 weeks postinfusion.<sup>23</sup> At 24 weeks, the serum levels of ALT and AST in AAV-PAL-injected mice returned to normal levels (Figures 4A and 4B). Moreover, histological examination of liver, kidney, heart, spleen, and lung sections did not detect obvious morphological abnormalities (Figure 4C).

Next, we tested whether *trans*-cinnamic acid produced by PAL was further metabolized in liver or secreted into blood. A high-performance liquid chromatography (HPLC) examination revealed that no detectable *trans*-cinnamic acid was observed in all treated mice. To confirm our examination, we used the same experimental setting to examine *trans*-cinnamic acid in the culture media from PAL-transfected 293T or HepG2 cells, and we did observe a significant level of *trans*-cinnamic acid in those media (Figure 4D). These results suggested that most *trans*-cinnamic acids produced by transgenic PAL were further metabolized. In supporting this notion, we detected considerable hippuric acid excretion from the urea of PAL-treated mice. No hippuric acid was detected in PBS-treated PKU mice (Figure S2). Importantly, the excretion levels were dependent on the dosages of PAL virus (Figures 4E and 4F).

Because the therapeutic transgene we used was derived from *Anabaena variabilis*, it is thus exogenous to mice; therefore, it is necessary to determine whether AAV-PAL mice developed an immune response to PAL. As shown in Figure 4G, we did not detect the presence of PAL antibody in the serum of mice injected with the highest dosage of AAV-PAL at 2 and 4 weeks after AAV infusion, nor did we detect any elevation in the level of serum interferon- $\gamma$  (IFN- $\gamma$ ) in AAV-PAL-injected mice (Figure 4H). Together with the results from hepatotoxicity testing, these observations demonstrated the safety of AAV-PAL gene therapy.

## DISCUSSION

Early identification of PKU through neonatal screening can direct lifesaving intervention before development of HPA-related syn-

drome.<sup>3</sup> Currently, nutritional management is an essential intervention for PKU treatment, consisting in a semi-synthetic and low-Phe diet, which includes measured amounts of lower protein foods and Phe-low protein substitutes.<sup>24</sup> However, dietary intervention involves a major alteration of normal lifestyle and can also be associated with deficiencies of other necessary nutrients.<sup>25</sup>

Recently, AAV-mediated PAH gene therapies have achieved significant restoration of liver PAH activity and reduction of Phe levels in PKU mouse models. However, a gender difference was observed in most reports.<sup>6–10</sup> Although AAV8-PAH treatment resulted in nearly complete and long-term correction of HPA and reversal of HPA-related syndromes in male mice, achieving long-term therapeutic effects in females remains challenging, possibly because of low infection efficiency of AAV in female mice.<sup>26</sup> In addition, low endogenous BH4 levels in female mice may also contribute to gender-dependent response to PAH gene therapy.<sup>13</sup>

In addition to PAH gene therapy, enzyme substitution therapy with non-mammalian-derived PAL proteins achieved correction of HPA and reversal of HPA-related syndrome in both animal models and PKU patients.<sup>14–18</sup> Unlike PAH, PALs do not require any coenzymes when catalyzing the reaction, in which Phe is converted into *trans*-cinnamic acid (TCA) and trace amounts of ammonia.<sup>11,12</sup> Ammonia is a common metabolite that occurred in various inherent deamination reactions. *Trans*-cinnamate is further converted in the liver into benzoic acid and excreted in the urine mainly as Hippurate.<sup>27</sup> Therefore, theoretically, PAL substitution therapy caused low toxic effects, making it a good candidate for PAH substitution. Consistent with this notion, subcutaneous administration of PAL in PKU animal models significantly reduced blood Phe level, reversed PKU-associated hypopigmentation, and enhanced animal health. However, because enzyme substitution therapy requires repeated lifelong injection of exogenous proteins, both immune response and patient compliance are big challenges.<sup>21,22</sup> Besides, under a normal diet, a once-weekly dosage of PAL protein was not able to stably reduce Phe level. Blood Phe was significantly reduced during the day of PAL injection and finally raised to the level before the next injection as high as that in untreated controls, which was possibly due to a short half-life of PAL proteins, impeding its implication in infants.<sup>17,19,28</sup>

To address these problems, we sought to express PAL in cells to achieve a more stable expression than protein injection does. Transgenic expression with AAV gene therapy is a good choice. The first hurdle in the way of this strategy was whether intracellularly expressed PAL could efficiently reduce extracellular Phe level while not damaging its host cells. We expressed PAL in mammalian cells

### Figure 2. A Single Dose of AAV8-PAL Corrected Hyperphenylalaninemia in Male PKU Mice

(A) Schematic diagram showing the structure and delivery of AAV8-PAL vector. (B) Time course of blood Phe levels following AAV8-PAL injection. Three PKU male mice were injected with the indicated dosage of AAV8-PAL via tail vein, and blood Phe levels were measured bi-weekly thereafter. PKU mice that received PBS injection served as negative control (data are represented as mean  $\pm$  SD). (C) Hair color recovery in male mice received  $4 \times 10^{12}$  viral particles at 0, 2, 8, and 24 weeks postinjection. Mice that received lower dosages did not show obvious color recovery. (D) Immunohistochemistry detecting PAL expression in liver tissue from PKU male mice received treatment as indicated (high-magnification scale bars, 100  $\mu$ m; low-magnification scale bars, 200  $\mu$ m).

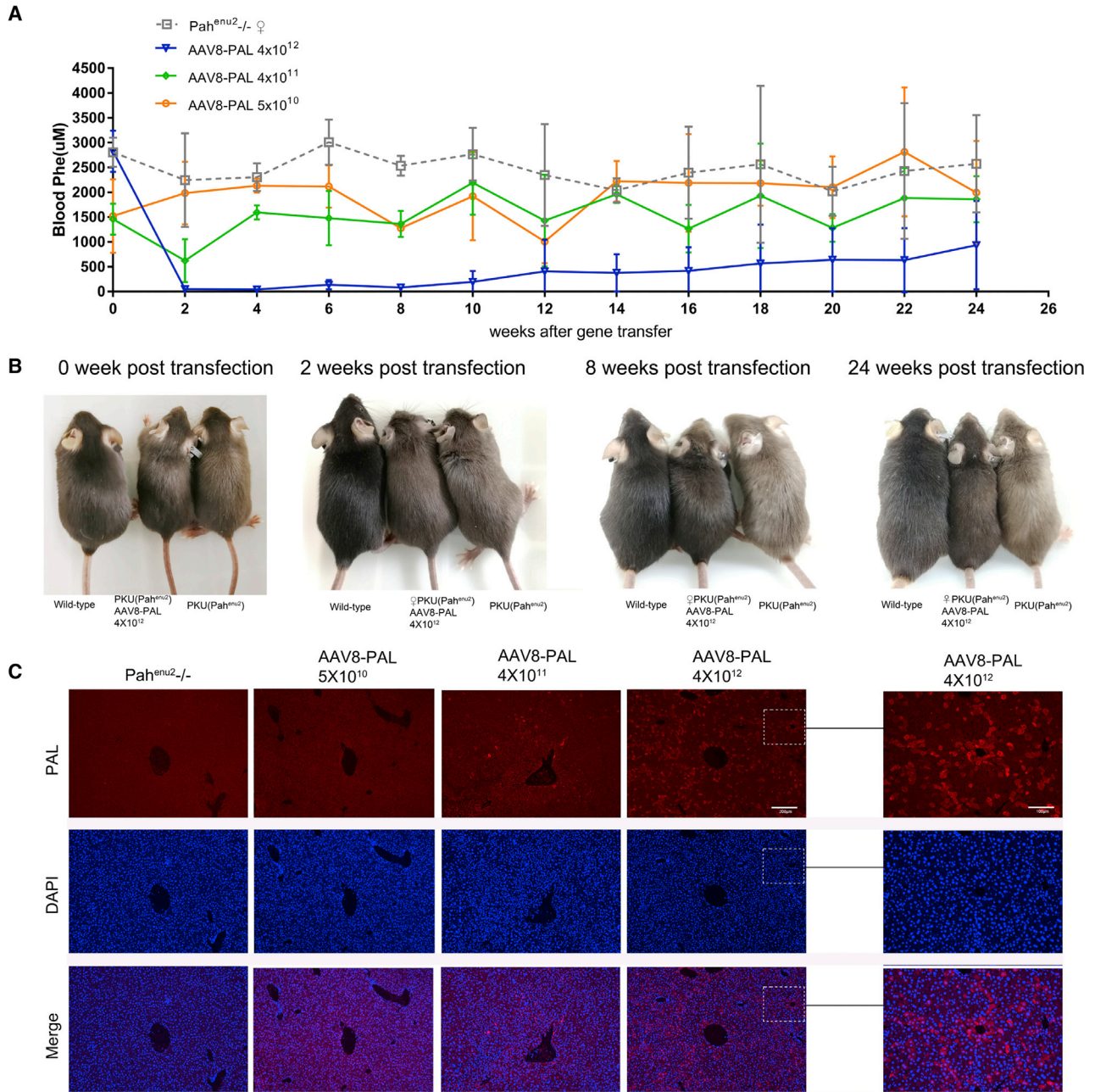


**Figure 3. A Single Dose of AAV8-PAL Corrected Hyperphenylalaninemia in Female PKU Mice**

(A) Time course of blood Phe levels following AAV8-PAL injection. Three PKU female mice received AAV8-PAL via tail vein with indicated dosages, and blood Phe levels were measured bi-weekly thereafter. PKU mice that received PBS injection served as negative control (data are represented as mean  $\pm$  SD). (B) Hair color recovery in female mice received  $4 \times 10^{12}$  viral particles at 0, 2, 8, and 24 weeks postinjection. Mice that received lower dosages did not show obvious color recovery. (C) Immunohistochemistry detecting PAL expression in liver tissue from PKU female mice received treatment as indicated (high-magnification scale bars, 100  $\mu$ m; low-magnification scale bars, 200  $\mu$ m).

and observed significant clearance of extracellular Phe, suggesting the potential of PAL in gene therapy. We then expressed PAL in the liver of PKU mice by introducing recombinant AAV (rAAV) expressing the humanized PAL under the control of liver-specific hAAT pro-

motor. Our results showed that a single intravenous administration of AAV8-PAL caused long-term correction of HPA in both male and female PKU mice. As early as 2 weeks after AAV8-PAL administration, the blood Phe level was dramatically reduced from



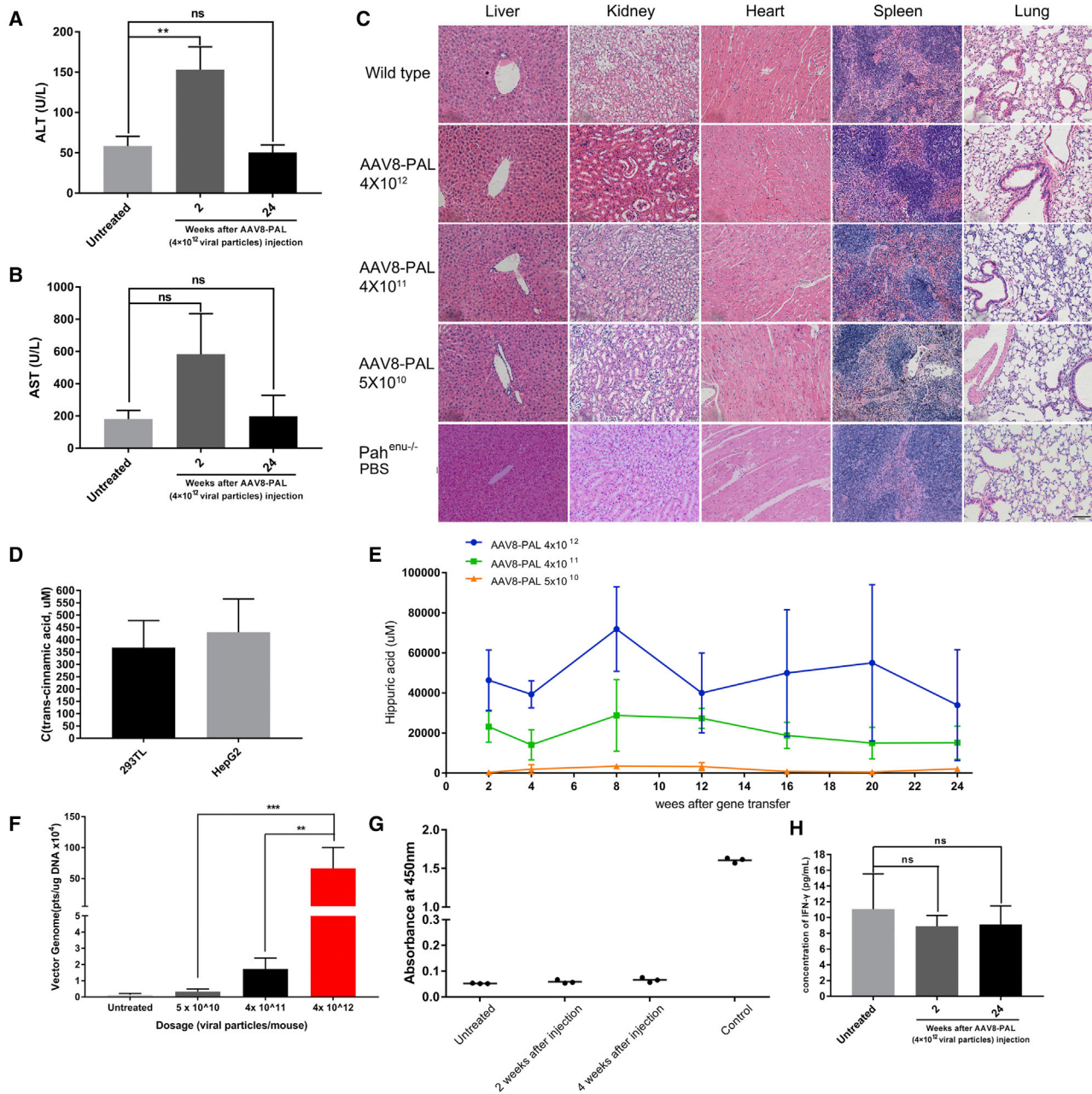


**Figure 4. Safety Evaluation of AAV8-PAL Treatment**

(A and B) ALT (A) and AST (B) testing in AAV8-PAL-treated PKU mice. After 2 and 24 weeks of AAV8-PAL treatment, serum ALT and AST levels were measured in PKU mice that received  $4 \times 10^{12}$  viral particles ( $n = 3$ , 1 male and 2 females). Wild-type healthy mice were used as normal control. (C) Tissue section and H&E staining of main parenchymal organs, including liver, kidney, heart, spleen, and lung. No obvious morphological abnormality and inflammatory cell infiltration were found in these organs (scale bars, 100  $\mu\text{m}$ ). (D) Detection of *trans*-cinnamic acid in culture medium conditioned with PAL expression (data are represented as mean  $\pm$  SD). (E) Detection of hippuric acid content in urine of AAV8-PAL-treated mice ( $n = 3$  in each group, data are represented as mean  $\pm$  SD). (F) rAAV genome copies in liver cells (24 weeks postinjection, each group contained 2 male and 2 female mice; data are represented as mean  $\pm$  SD; \* $p < 0.05$ ). (G) Antibody against PAL protein was not detected in mice treated with AAV8-PAL ( $4 \times 10^{12}$  viral particles) at 2 and 4 weeks postinjection compared with untreated control mice. Antibody raised from rabbit served as positive control ( $n = 3$  in each group, 1 male, 2 females; data are represented as mean  $\pm$  SD; \* $p < 0.05$ ). (H) Serum of AAV8-PAL ( $4 \times 10^{12}$  viral particles)-treated mice was collected and measured for IFN- $\gamma$  level by ELISA ( $n = 3$ , 1 male, 2 females; data are represented as mean  $\pm$  SD).

2,708 ± 849 μM to lower than 120 μM in the 4 × 10<sup>12</sup> viral particles group and in a gender-independent manner. In most cases (four out of six), low Phe levels were maintained during the whole experimental period of at least 24 weeks (Tables S1 and S2), accompanied with a nearly complete reversal of HPA-associated hypopigmentation. In the other two cases, their blood Phe level began to rise at about 12 weeks after administration and stabilized at 40% or 60% of the pre-treatment concentration, which was likely due to individual differences.

Safety issues are big concerns during therapeutic designs. As mentioned above, the main product of PAL catalyzation, *trans*-cinnamic acid, is metabolized in the liver; therefore, we chose liver as our target organ. Consistent with previous reports about *trans*-cinnamic acid metabolism, we observed a significant level of Hippurate in the urine of PAL-treated mice in a dose-dependent manner. Besides, liver function testing revealed that AAV8-PAL administration did not result in any detectable liver damage. Also, no morphological abnormality in other organs was detected, suggesting that *trans*-cinnamic acid did not accumulate in and cause damage to the liver and other organs. Taken together, our results demonstrated that PAL-based gene therapy is a promising option in the treatment of PKU syndrome.

## MATERIALS AND METHODS

### Materials

Dulbecco's modified Eagle's medium (DMEM) and penicillin-streptomycin were purchased from Thermo Fisher Scientific. TransIT-2020 (Mirus) was used to transfer foreign genes into cells, and the Phe assay kit was manufactured by Guangzhou Fenghua Bioengineering. Phe standard and TCA standard were purchased from Sigma, and hippuric acid standard was from Solarbio. PAL antibody was produced against the N terminus of PAL protein by ABclonal. Mouse IFN-γ enzyme-linked immunosorbent assay (ELISA) assay was purchased from BioLegend.

### Cell Culture and Transfection

293T and HepG2 cell lines were maintained in DMEM, supplemented with 10% (v/v) FBS and 1 × penicillin-streptomycin at 37°C and 5% CO<sub>2</sub>. The cells were seeded on 24-well cell culture plates and transfected using 1.5 μL TransIT-2020 according to the manufacturer's protocol. When the cells grew approximately 70% confluency at 24 h after seeding, 0.5 μg plasmid DNA was transfected for pCMV-AvPAL.

### Animals

The B6.BTBR-Pah<sup>enu2</sup> mouse model purchased from Jackson Laboratory carries a missense mutation (c.835T → C) in exon 7 (p.F263S) of the *Pah* gene. Developing homozygous *Pah*<sup>enu2-/-</sup> and *Pah*<sup>enu2+/-</sup> (WT) mice were issued from heterozygous mating *Pah*<sup>enu2+/-</sup>. Animals were housed in specific pathogen-free (SPF) animal breeding rooms and maintained on a 12-h light/dark cycle. All mice were provided with standard laboratory chow and water. All animal procedures were performed following the protocol approved by the

Institutional Animal Care and Treatment Committee of Sichuan University (Chengdu, China).

### Design of the rAAV Vector

The plasmid construct AAV8-PAL, which directs the expression of PAL from a liver-specific hAAT/ApoE, has been described previously.<sup>29</sup> The PAL expression cassettes were subsequently tested for expression after packaging in single-strand AAV vectors.

All rAAV8 vectors were produced at Sichuan University, using a triple-transfection protocol as previously described.<sup>30</sup> Vectors were produced by transient transfection of HEK293 cells, purified from clarified cell lysates by two rounds of cesium chloride density gradient centrifugations, and diafiltrated into an isotonic formulation. Next, the AAV vectors were tested in quality-control assays that were designed to ensure its safety, efficiency, and stability, including titer determination by silver staining and quantitative polymerase chain reaction (qPCR).

### In Vivo Expression of PAL in the PKU Mouse Model

We investigated the expression and function of AAV8-PAL in PKU mice using rAAV vectors. The low-dosage group was injected with 5 × 10<sup>10</sup> viral particles per mouse. The middle-dosage group was administered 4 × 10<sup>11</sup> viral particles per mouse. The high-dosage group was administered 4 × 10<sup>12</sup> viral particles per mouse. Three male and three female mice in each group were injected (Table 1). The mice to be treated were numbered with ear tag pliers. Three doses of rAAV8 viral particles were diluted into 200 μL PBS and injected into 4- to 8-week-old PKU mice via tail veins, respectively.

### Measurement of Phe Concentration

For the cell culture medium, analysis of Phe was performed on LC-MS (QTRAP 5500; AB SCIEX) and HPLC (UFLC and LC-30AD; Shimadzu). All of the samples were injected into the liquid chromatography using a Waters HPLC BEH C18 column (2.1 × 50 mm, 1.7-μM particle size). The mobile phase (0.1% formic acid in water/methanol) was pumped at a flow rate of 0.5 mL/min. The mass spectrometry conditions were: ion detection method (multiple reaction mode), ion polarity (positive), declustering potential (120.0 V), entrance potential (10.0 V), collision energy (18.0 eV), collision cell exit potential (10.0 V), ion source (turbo spray), curtain gas (20.0 Psi), collision gas (medium), ionspray voltage (5,500.0 V), temperature (500.0°C), ion source gas 1 (60.0 Psi), and ion source gas 2 (60.0 Psi).

For blood samples, the blood was collected at 4 p.m. according to previous reports,<sup>18</sup> and the whole blood was collected on the blood specimen collection card, dried under ambient conditions, and stored at 4 p.m. in plastic bags. The concentration of Phe in the blood was tested by dry blood spots, according to the protocol provided in the Phe assay kit.

### Western Blot Analysis

Western blot assays were performed as previously described<sup>31</sup> with modification. Cell lysates were subjected to SDS-PAGE gel



**Table 1. Treatment Groups**

Dosage (Particles/Mouse)	Male				Female			
	Ear Tag	Age (Weeks)	Blood Phe ( $\mu\text{M}$ ) Weeks Postinjection		Ear Tag	Age (Weeks)	Blood Phe ( $\mu\text{M}$ ) Weeks Postinjection	
			0	24			0	24
$4 \times 10^{12}$	D56	5	3,683.3	1,224.1	D17	4	ND	1,814.1
	B25	4	2,137.1	58.3	F46	4	2,532.6	33.1
	B28	4	2,303.0	36.0	G198	5	3,118.0	953.2
$4 \times 10^{11}$	C46	6	1,302.2	ND	B14	8	1,784.5	2,365.9
	G123	4	1,882.3	1,567.8	H143	8	1,429.6	1,767.1
	G191	4	2,788.9	1,291.7	G158	6	1,158.8	1,448.9
$5 \times 10^{10}$	B19	8	2,324.6	1,897.0	C25	7	2,247.9	3,187.4
	C21	7	1,899.3	1,905.5	C84	7	1,550.6	1,312.5
	F81	4	711.1	870.2	F88	4	767.9	1,479.7
Untreated	D60	4	2,303.1	1,603.1	D91	4	2,762.6	3,022.5
	D98	6	2,137.1	1,670.6	M059	5	3,117.9	1,451.9
	D80	7	2,919.9	2,375.5	D92	6	2,532.6	3,250.9
p value			0.354	0.06			0.018	0.221

ND, not determined.

electrophoresis (ZOMANBIO) and blotted on polyvinylidene fluoride (PVDF) membranes (Immobilon-<sup>PSQ</sup>). The blots were probed with anti-PAL (1:1,000 dilution) and anti-GAPDH (Abcam; 1:1,000) primary antibodies, and then HRP-conjugated anti-Rabbit and anti-Mouse [1:2,000 dilution, Beyotime HRP Goat anti-rabbit and HRP Goat anti-mouse Ig (H+L)] secondary antibodies, respectively.

For the cell culture medium, all cells were incubated in complete fresh medium for 48 h after transfection. The complete medium was then replaced by serum-free medium (293 SMFII with 100 $\times$  GlutaMAX; Gibco) and incubated for 24 h. Next, the serum-free medium was subjected to western blot. The blots were probed with anti-PAL (1:1,000 dilution) and anti-vascular endothelial growth factor (anti-VEGF; 1:1,000; Abcam) primary antibodies, and then HRP-conjugated anti-Rabbit (1:2,000 dilution; Beyotime HRP Goat anti-rabbit) secondary antibody.

#### Immunofluorescence

The cells were fixed in 4% paraformaldehyde for 15 min at room temperature. Primary antibody to PAL (rabbit anti-PAL) was used at 1:500 dilution. The secondary antibody, Alexa Fluor 594 anti-rabbit (Proteintech), was used at a concentration of 1:200.

The liver samples were removed from mice immediately upon sacrifice and fixed in 0.1 M phosphate buffer (pH 7.4) containing 4% paraformaldehyde overnight at 4°C, and then embedded in paraffin and sectioned. Primary antibody to PAL (rabbit anti-PAL) was used at 1:500 dilution. The secondary antibody, Alexa Fluor 594-conjugated Goat anti-rabbit (Proteintech), was used at a concentration of 1:200.

#### Liver Function Test and Histological Examination

Aged mice were bled, and the sera were collected. Liver function tests were performed by West China Second University Hospital, Sichuan University.

After 2 and 24 weeks of treatment, the mice were sacrificed by cervical dislocation. The tissues were then fixed in 4% paraformaldehyde, embedded in paraffin, sectioned, and stained with hematoxylin and eosin.

#### HPLC Measurement of TCA

Analysis of TCA was performed on Waters HPLC 2695 series instrument with a 150/4.6 Waters SC18-MS-II column at 37°C. Chromatography was performed with a flow rate of 1.0 mL/min and injection volume of 10  $\mu\text{L}$ . Isocratic elution was performed with a mobile phase of 65% methanol, 35% H<sub>2</sub>O-acetic acid in purified water (pH 4.0). TCA was monitored at a wavelength of 280 nm with a retention time of 4.7–6.6 min.

#### Determination of Hippuric Acid in Urine by HPLC

Analysis of hippuric acid was performed on Waters HPLC 2695 series instrument with a 150/4.6 Waters SC18-MS-II column at 40°C. Chromatography was performed with a flow rate of 1.0 mL/min and injection volume of 10  $\mu\text{L}$ . Isocratic elution was performed with a mobile phase of 40% methanol, 60% phosphoric acid in purified water (pH 2.98). Hippuric acid was monitored at a wavelength of 228 nm with a retention time of 3–5 min.

#### Quantification of rAAV Genome Copy in Liver Cells

To quantify viral genome copies in liver cells, we isolated total genome DNA from the frozen liver tissues using the TIANamp

Genomic DNA Kit (TIANGEN, Beijing, China). Viral genomes were quantified by qPCR using TransStart Tip Green qPCR SuperMix (Transgen Biotech, Beijing, China) using StepOnePlus Real-Time PCR System (Applied Biosystems, Carlsbad, CA, USA). The titers of viral genomes were detected by qPCR (Transgen Biotech, Beijing, China). In a 20- $\mu$ L qPCR system, 100 ng of genome DNA for each sample was used as the template, and the primer pairs were the same as above for detection of AAV titration, AAV Forward: 5'-TGCCGACCAAATGATTAGCC-3' and AAV Reverse: 5'-CCACGATGGGTCCAAGGTATT-3'. Data were normalized to mouse glyceraldehyde-3-phosphate dehydrogenase (mGAPDH), and primer pairs used for mGAPDH were mGAPDH Forward: 5'-AACG GATTTGGCCGATTGG-3' and mGAPDH Reverse: 5'-CATTCT CGGCCTTGACTGTG-3'.

### ELISA

For serum anti-PAL antibody detection, antigen, the purified PAL protein, was coated onto a 96-well MaxiSorp plate (Costar) overnight at 4°C in 1 $\times$  coating buffer (0.05 M sodium carbonate-sodium bicarbonate [pH 9.6]). Plates were then washed three times for 5 min on a shaker with 1 $\times$  wash buffer (PBST [pH 8.0]). Plates were then blocked with blocking solution (PBST with 5% bovine serum albumin) for 2 h at 37°C. Serum samples were applied diluted in blocking solution at varying concentrations as described for each experiment. Plates were incubated for 2 h at 37°C. Plates were then washed as described previously, and horseradish peroxidase (HRP)-conjugated goat anti-mouse antibody (Beyotime) was then applied at a dilution of 1:250 in blocking solution and incubated for 2 h at 37°C. 3,3',5,5'-Tetramethylbenzidine substrate solution (Solarbio) was then added and allowed to develop for 15 min before 1N sulfuric acid was added to stop the reaction. The absorbance at 450 nm was then analyzed using a microplate reader.

The levels of serum IFN- $\gamma$  (pg/mL) were measured using a microplate reader and were calculated according to an IFN- $\gamma$  standard curve supplied in the kits. Levels of IFN- $\gamma$  were measured using a mouse IFN- $\gamma$  ELISA kit (BioLegend). All samples were tested in duplicate according to the manufacturer's instructions.

### Statistics

Statistical tests were performed using SPSS (version 11.5). A  $p$  value  $<0.05$  was considered statistically significant. \*\*\*\* $p < 0.0001$ , \*\*\* $p < 0.001$ , \*\* $p < 0.01$ , \* $p < 0.05$ , <sup>ns</sup> $p > 0.05$ .

Based on the number of tested groups for comparison, the levels of significance were determined by appropriate statistical analysis. Independent sample  $t$  test was used to determine levels of significance for comparisons between two groups, one-way ANOVA test was performed to analyze the difference among groups, and data were presented as mean  $\pm$  SD.

### SUPPLEMENTAL INFORMATION

Supplemental Information can be found online at <https://doi.org/10.1016/j.omtm.2019.12.014>.

### AUTHOR CONTRIBUTIONS

B.D. and S.Y. developed the concept and prepared the manuscript. R.T. and L.X. designed and performed the experiments, including cell culture and transfection, animal breeding, AAV8 vector construction and purification, sample collection and testing, data organization, statistical analyses, and the manuscript preparation. Lifang Zhou, Z.Z., J.L., and Lixing Zhou grew cells, bred animals, and collected and tested samples. M.T. processed and tested the cell medium and blood samples. All authors read and approved the final manuscript.

### CONFLICTS OF INTEREST

The authors declare no competing interests.

### ACKNOWLEDGMENTS

This research was supported by National Natural Science Foundation of China (No. 81974238, No. 81571792 and U19A2002), Salubris Academician Workstation for Innovative Biopharmaceuticals (No. 2017B090904017) and Project for Disciplines of Excellence, West China Hospital, Sichuan University (No. ZY2017201).

### REFERENCES

1. Ho, G., and Christodoulou, J. (2014). Phenylketonuria: translating research into novel therapies. *Transl. Pediatr.* 3, 49–62.
2. Scriver, C.R., and Kaufman, S. (2001). Hyperphenylalaninemia: phenylalanine hydroxylase deficiency. In *The Metabolic and Molecular Bases of Inherited Disease*, Eighth Edition, C.R. Scriver, A.L. Beauder, S.W. Sly, and et al., eds. (McGraw-Hill), pp. 1667–1724.
3. Guthrie, R., and Susi, A. (1963). A Simple Phenylalanine Method for Detecting Phenylketonuria in Large Populations of Newborn Infants. *Pediatrics* 32, 338–343.
4. Evans, S., Daly, A., MacDonald, J., Preece, M.A., Santra, S., Vijay, S., Chakrapani, A., and MacDonald, A. (2014). The micronutrient status of patients with phenylketonuria on dietary treatment: an ongoing challenge. *Ann. Nutr. Metab.* 65, 42–48.
5. Mochizuki, S., Mizukami, H., Ogura, T., Kure, S., Ichinohe, A., Kojima, K., Matsubara, Y., Kobayashi, E., Okada, T., Hoshika, A., et al. (2004). Long-term correction of hyperphenylalaninemia by AAV-mediated gene transfer leads to behavioral recovery in phenylketonuria mice. *Gene Ther.* 11, 1081–1086.
6. Ding, Z., Georgiev, P., and Thöny, B. (2006). Administration-route and gender-independent long-term therapeutic correction of phenylketonuria (PKU) in a mouse model by recombinant adeno-associated virus 8 pseudotyped vector-mediated gene transfer. *Gene Ther.* 13, 587–593.
7. Rebuffat, A., Harding, C.O., Ding, Z., and Thöny, B. (2010). Comparison of adeno-associated virus pseudotype 1, 2, and 8 vectors administered by intramuscular injection in the treatment of murine phenylketonuria. *Hum. Gene Ther.* 21, 463–477.
8. Yagi, H., Ogura, T., Mizukami, H., Urabe, M., Hamada, H., Yoshikawa, H., Ozawa, K., and Kume, A. (2011). Complete restoration of phenylalanine oxidation in phenylketonuria mouse by a self-complementary adeno-associated virus vector. *J. Gene Med.* 13, 114–122.
9. Harding, C.O., Gillingham, M.B., Hamman, K., Clark, H., Goebel-Daghighi, E., Bird, A., and Koeberl, D.D. (2006). Complete correction of hyperphenylalaninemia following liver-directed, recombinant AAV2/8 vector-mediated gene therapy in murine phenylketonuria. *Gene Ther.* 13, 457–462.
10. Laipis, P.J., Charron, C.E., Embury, J.E., Perera, O.P., Porvasnik, S.L., Fields, C.R., and Zori, R.T. (2004). Correction of maternal phenylketonuria syndrome in the Pah<sup>enu2</sup> missense mutant mouse by r-AAV mediated gene therapy. *Mol. Ther.* 9 (Suppl 1), S334.
11. Scriver, C.R. (1971). Mutants: consumers with special needs. *Nutr. Rev.* 29, 155–158.

12. Koukol, J., and Conn, E.E. (1961). The metabolism of aromatic compounds in higher plants. IV. Purification and properties of the phenylalanine deaminase of *Hordeum vulgare*. *J. Biol. Chem.* 236, 2692–2698.
13. MacDonald, M.J., and D’Cunha, G.B. (2007). A modern view of phenylalanine ammonia lyase. *Biochem. Cell Biol.* 85, 273–282.
14. Gámez, A., Sarkissian, C.N., Wang, L., Kim, W., Straub, M., Patch, M.G., Chen, L., Striepeke, S., Fitzpatrick, P., Lemontt, J.F., et al. (2005). Development of pegylated forms of recombinant *Rhodospiridium toruloides* phenylalanine ammonia-lyase for the treatment of classical phenylketonuria. *Mol. Ther.* 11, 986–989.
15. Ikeda, K., Schiltz, E., Fujii, T., Takahashi, M., Mitsui, K., Kodera, Y., Matsushima, A., Inada, Y., Schulz, G.E., and Nishimura, H. (2005). Phenylalanine ammonia-lyase modified with polyethylene glycol: potential therapeutic agent for phenylketonuria. *Amino Acids* 29, 283–287.
16. Gámez, A., Wang, L., Sarkissian, C.N., Wendt, D., Fitzpatrick, P., Lemontt, J.F., Scriver, C.R., and Stevens, R.C. (2007). Structure-based epitope and PEGylation sites mapping of phenylalanine ammonia-lyase for enzyme substitution treatment of phenylketonuria. *Mol. Genet. Metab.* 91, 325–334.
17. Sarkissian, C.N., Gámez, A., Wang, L., Charbonneau, M., Fitzpatrick, P., Lemontt, J.F., Zhao, B., Vellard, M., Bell, S.M., Henschell, C., et al. (2008). Preclinical evaluation of multiple species of PEGylated recombinant phenylalanine ammonia lyase for the treatment of phenylketonuria. *Proc. Natl. Acad. Sci. USA* 105, 20894–20899.
18. Zeile, W.L., McCune, H.C., Musson, D.G., O’Donnell, B., O’Neill, C.A., Tsuruda, L.S., Zori, R.T., and Laipis, P.J. (2018). Maternal phenylketonuria syndrome: studies in mice suggest a potential approach to a continuing problem. *Pediatr. Res.* 83, 889–896.
19. Sarkissian, C.N., Kang, T.S., Gámez, A., Scriver, C.R., and Stevens, R.C. (2011). Evaluation of orally administered PEGylated phenylalanine ammonia lyase in mice for the treatment of Phenylketonuria. *Mol. Genet. Metab.* 104, 249–254.
20. Gupta, S., Lau, K., Harding, C.O., Shepherd, G., Boyer, R., Atkinson, J.P., Knight, V., Olbertz, J., Larimore, K., Gu, Z., et al. (2018). Association of immune response with efficacy and safety outcomes in adults with phenylketonuria administered pegvaliase in phase 3 clinical trials. *EBioMedicine* 37, 366–373.
21. Lubich, C., Allacher, P., de la Rosa, M., Bauer, A., Prenninger, T., Horling, F.M., Siekmann, J., Oldenburg, J., Scheiflinger, F., and Reipert, B.M. (2016). The Mystery of Antibodies Against Polyethylene Glycol (PEG)—What do we Know? *Pharm. Res.* 33, 2239–2249.
22. Verhoef, J.J., Carpenter, J.F., Anchordoquy, T.J., and Schellekens, H. (2014). Potential induction of anti-PEG antibodies and complement activation toward PEGylated therapeutics. *Drug Discov. Today* 19, 1945–1952.
23. Wang, L., Wang, H., Bell, P., McCarter, R.J., He, J., Calcedo, R., Vandenberghe, L.H., Morizono, H., Batshaw, M.L., and Wilson, J.M. (2010). Systematic evaluation of AAV vectors for liver directed gene transfer in murine models. *Mol. Ther.* 18, 118–125.
24. MacDonald, A., Gokmen-Ozel, H., van Rijn, M., and Burgard, P. (2010). The reality of dietary compliance in the management of phenylketonuria. *J. Inherit. Metab. Dis.* 33, 665–670.
25. Demirkol, M., Gizewska, M., Giovannini, M., and Walter, J. (2011). Follow up of phenylketonuria patients. *Mol. Genet. Metab.* 104 (Suppl), S31–S39.
26. Ho, K.J., Bass, C.E., Kroemer, A.H., Ma, C., Terwilliger, E., and Karp, S.J. (2008). Optimized adeno-associated virus 8 produces hepatocyte-specific Cre-mediated recombination without toxicity or affecting liver regeneration. *Am. J. Physiol. Gastrointest. Liver Physiol.* 295, G412–G419.
27. Blau, N., and Longo, N. (2015). Alternative therapies to address the unmet medical needs of patients with phenylketonuria. *Expert Opin. Pharmacother.* 16, 791–800.
28. Kang, T.S., Wang, L., Sarkissian, C.N., Gámez, A., Scriver, C.R., and Stevens, R.C. (2010). Converting an injectable protein therapeutic into an oral form: phenylalanine ammonia lyase for phenylketonuria. *Mol. Genet. Metab.* 99, 4–9.
29. Le, M., Okuyama, T., Cai, S.R., Kennedy, S.C., Bowling, W.M., Flye, M.W., and Ponder, K.P. (1997). Therapeutic levels of functional human factor X in rats after retroviral-mediated hepatic gene therapy. *Blood* 89, 1254–1259.
30. Dong, B., Moore, A.R., Dai, J., Roberts, S., Chu, K., Kapranov, P., Moss, B., and Xiao, W. (2013). A concept of eliminating nonhomologous recombination for scalable and safe AAV vector generation for human gene therapy. *Nucleic Acids Res.* 41, 6609–6617.
31. Abou-Hashem, M.M.M., Abo-Elmatty, D.M., Mesbah, N.M., and Abd El-Mawgoud, A.M. (2019). Induction of sub-G<sub>0</sub> arrest and apoptosis by seed extract of *Moringa peregrina* (Forssk.) Fiori in cervical and prostate cancer cell lines. *J. Integr. Med.* 17, 410–422.



**OMTM, Volume 19**

**Supplemental Information**

**Long-Term Metabolic Correction  
of Phenylketonuria by AAV-Delivered  
Phenylalanine Amino Lyase**

**Rui Tao, Lin Xiao, Lifang Zhou, Zhaoyue Zheng, Jie Long, Lixing Zhou, Minghai Tang, Biao Dong, and Shaohua Yao**

## Supplementary Material

Table S1. Blood Phe of AAV8-PAL-treated males.

Weeks after gene transfer	Blood Phe of males ( $\mu\text{M}$ )								
	$4 \times 10^{12}$			$4 \times 10^{11}$			$5 \times 10^{10}$		
	D56	B25	B28	C46	G123	G191	B19	C21	F81
0	3683.3	2137.1	2303.0	1302.2	1882.3	2788.9	2324.6	1899.3	711.1
2	31.1	30.2	36.1	736.8	2078.2	932.1	.	1538.1	1895.0
4	52.1	48.0	72.7	1186.8	2547.6	1853.0	.	1644.3	1605.7
6	69.2	92.5	30.1	1874.1	1915.6	2144.5	1539.4	.	2005.4
8	150.3	70.7	62.2	.	2187.8	934.1	1298.4	.	1695.6
10	83.6	36.5	36.4	1403.9	2276.8	1310.8	1048.6	3075.4	1942.3
12	189.1	75.5	74.8	.	2220.3	687.9	822.5	.	1620.0
14	672.2	15.2	27.2	2017.8	3253.2	1084.5	1803.5	1299.6	1219.2
16	1186.2	103.8	26.7	889.4	1558.9	653.7	1865.4	1037.0	1715.1
18	1400.4	73.5	27.2	1720.6	736.3	1191.9	1949.5	1512.8	2879.3
20	1520.8	83.7	9.6	1888.0	2243.3	1074.2	1829.9	1474.6	618.6
22	1409.6	104.8	72.3	1193.1	1950.7	1585.6	1042.7	2198.4	1873.0
24	1224.1	58.3	36.0	.	1567.8	1291.7	1897.0	1905.5	870.2
52			384.8						

Table S2. Blood Phe of AAV8-PAL-treated females.

Weeks after gene transfer	Blood Phe of females ( $\mu\text{M}$ )								
	$4 \times 10^{12}$			$4 \times 10^{11}$			$5 \times 10^{10}$		
	D17	G198	F46	G158	H143	B14	C25	C84	F88
0	.	2532.6	3118.0	1784.5	1429.6	1158.8	2247.9	1550.6	767.9
2	.	52.3	41.3	926.6	317.9	.	1538.1	.	2428.0
4	40.2	27.6	53.8	1493.4	1694.3	.	2033.0	.	2232.4
6	249.2	74.6	93.7	1628.1	1940.7	870.4	.	2414.7	1814.0
8	73.6	103.2	63.3	1549.4	1177.7	.	.	1261.5	1290.5
10	454.6	52.2	78.9	2818.4	2227.3	1531.9	2943.1	1352.0	1465.0
12	1149.8	2.6	70.2	823.8	2493.5	967.5	.	698.4	1317.3
14	808.7	199.1	124.4	1926.5	1804.2	2148.3	1750.2	2480.6	2436.3
16	960.8	51.3	239.9	1230.5	808.1	1759.5	1476.1	1781.9	3308.5
18	1472.0	53.7	175.1	928.3	1834.9	3027.2	1924.1	1916.8	2702.1
20	1276.3	3.1	639.6	1396.8	963.7	1490.9	2530.0	2385.2	1389.9
22	1346.5	78.3	472.2	2522.3	1817.1	1309.6	2705.7	1568.0	4159.0
24	1814.1	33.1	953.2	2365.9	1767.1	1448.9	3187.4	1312.5	1479.7

Table S3. Blood Phe of wild-type mouse.

	Blood Phe of wild-type ( $\mu\text{M}$ )	
	♂	♀
	74.48	75.6
	93.94	124.03
	116.68	65.56
	97.86	196.92
	194.65	152.79
	114.23	144.53
	151.88	150.96
	125.71	209.12
	112.4	129.34
	65.15	103.48
	168.54	144.4
	49.4	52.33
	51.66	85.12
	86.03	137.14
	125.71	146.98
	49.33	56.03
	60.45	74.86
	46.67	93.16
	74.48	133.15
		168.94
		80.23
		58.17
		57.73
		154.44
		80.23
		70.37
		75.6
		124.03
N	18	26
Mean	99.1539	113.2931
Std. Deviation	43.567	45.598



Table S4. Serum ALT of wild-type mouse and AAV8-PAL-treated ( $4 \times 10^{12}$  viral particles) mouse

	ALT (U/L)		
	WT	2 weeks after injection	24 weeks after injection
	71	124	43
	47	154	47
	57	181	61
N	3(♂1 ♀2)	3(♂1 ♀2)	3(♂1 ♀2)
Mean $\pm$ SD	58.333 $\pm$ 12.055	153 $\pm$ 28.513	50.333 $\pm$ 9.452
P		0.006	0.417

Table S5. Serum AST of wild-type mouse and AAV8-PAL-treated ( $4 \times 10^{12}$  viral particles) mouse

	AST (U/L)		
	WT	2 weeks after injection	24 weeks after injection
	175	413	103
	237	464	143
	131	872	347
N	3(♂1 ♀2)	3(♂1 ♀2)	3(♂1 ♀2)
Mean $\pm$ SD	181 $\pm$ 53.254	583 $\pm$ 251.577	197.667 $\pm$ 130.864
P		0.104	0.848

Table S6. Serum IFN- $\gamma$  of wild-type mouse and AAV8-PAL-treated ( $4 \times 10^{12}$  viral particles) mouse

	IFN- $\gamma$ (pg/mL)		
	Untreated	2 weeks after injection	24 weeks after injection
	8.111	8.333	11.778
	8.889	10.444	7.333
	16.222	7.889	8.222
N	3(♂1 ♀2)	3(♂1 ♀2)	3(♂1 ♀2)
Mean $\pm$ SD	11.074 $\pm$ 4.475	8.889 $\pm$ 1.365	9.111 $\pm$ 2.352
P		0.464	0.538

Table S7. Anti-PAL antibody production

	untreated			2 weeks			4 weeks			control
Absorbance at 450nm	0.051	0.051	0.052	0.053	0.053	0.066	0.057	0.065	0.074	1.617
	0.051	0.051	0.054	0.053	0.056	0.066	0.057	0.065	0.074	1.57
	0.054	0.054	0.054	0.055	0.062	0.069	0.057	0.067	0.077	1.633
Mean	0.052	0.052	0.053	0.054	0.057	0.067	0.057	0.066	0.075	1.61

\*n = 3 per group

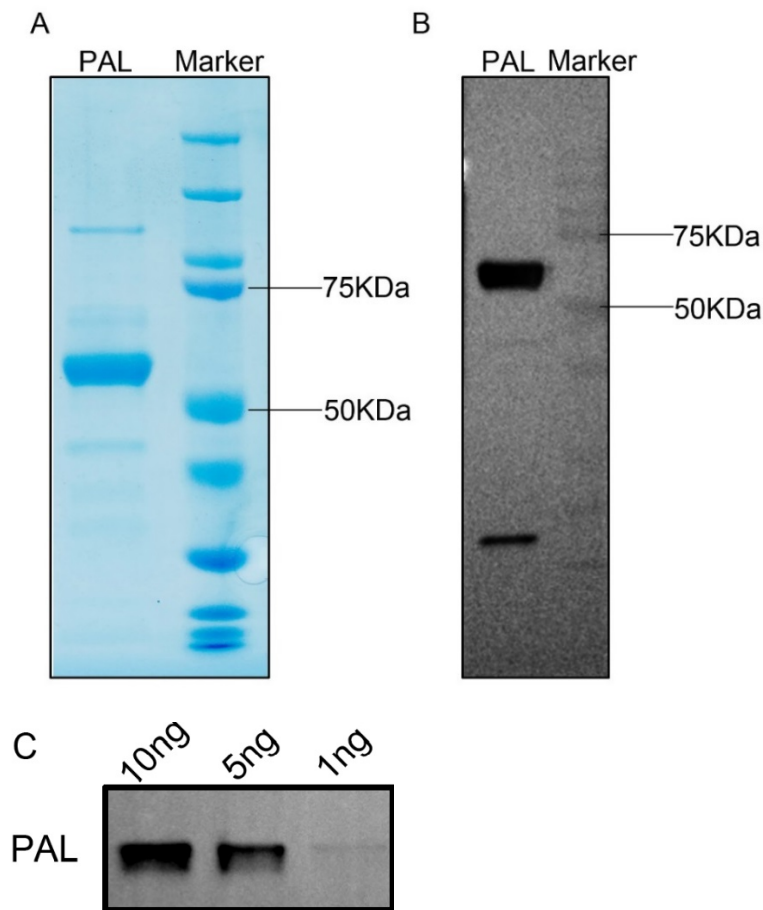


Figure S1. Testing of PAL anti-body. (A) Purified PAL was separated on a 10% SDS-PAGE gel and stained with Coomassie blue. (B)(C) Western blotting characterization of PAL protein expressed in *E. coli*.

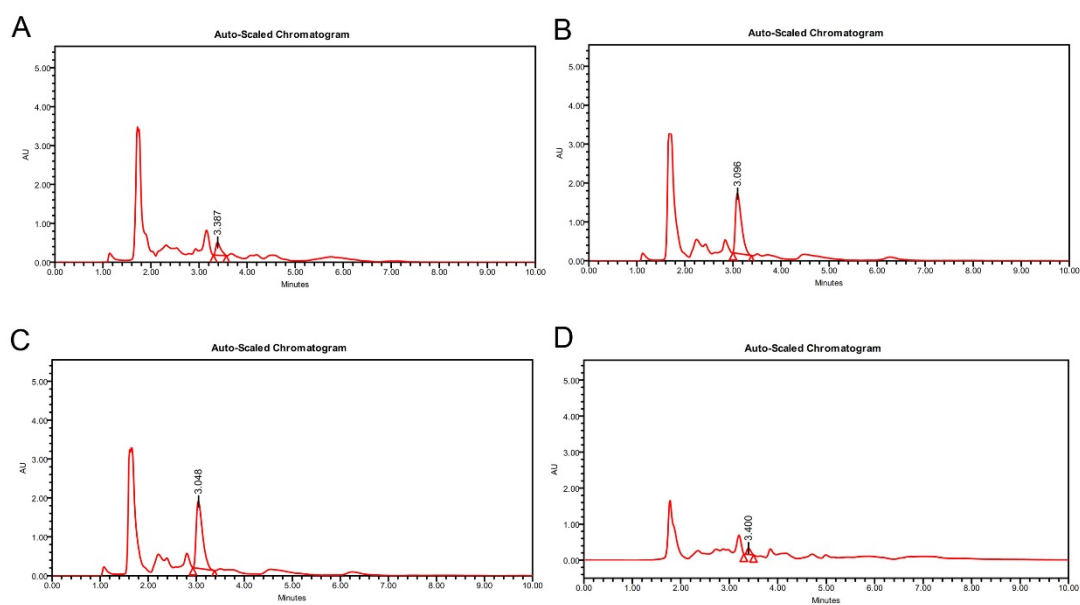


Figure S2. HPLC chromatogram of the hippuric acid standard solution (A) 0 $\mu$ M (B) 112 $\mu$ M (C) 558 $\mu$ M and (D) representative urine sample of PBS-treated mice.

Hippuric acid was monitored at a wavelength of 228nm. To balance the effects of other urinary materials that either have absorption at 280nm or affect the retention time of hippuric acid, urine from healthy control mice were used to dilute the samples and the standard solutions.